

## Focusing of nonducted whistlers by the equatorial anomaly

Vikas S. Sonwalkar and Umran S. Inan

Space, Telecommunications, and Radioscience Laboratory, Stanford University, Stanford, California

T. L. Aggson, W. M. Farrell, and R. Pfaff

NASA Goddard Space Flight Center, Greenbelt, Maryland

**Abstract.** Impulsive ELF/VLF electric field bursts observed by the vector electric field instrument (VEFI) on the Dynamics Explorer 2 (DE 2) satellite on almost every crossing of the geomagnetic equator in the evening hours are interpreted as originating in lightning discharges. These signals that peak in intensity near the magnetic equator are observed within 5-20° latitude of the geomagnetic equator at altitudes of 300-500 km with amplitudes of the order of  $\sim$  mV/m in the 512- to 1024-Hz frequency band of the VEFI instrument. Whistler-mode ELF/VLF wave propagation through a horizontally stratified ionosphere predicts strong attenuation of subionospheric signals reaching the equator at low altitudes. However, ray tracing analysis shows that the presence of the equatorial density anomaly, commonly observed in the upper ionosphere during evening hours, leads to the focusing of the wave energy from lightning near the geomagnetic equator at low altitudes, thus accounting for all observed aspects of the phenomenon. The observations presented here indicate that during certain hours in the evening, almost all the energy input from lightning discharges entering the ionosphere at  $<30^\circ$  latitude remains confined to a small region (in altitude and latitude) near the geomagnetic equator. The net wideband electric field, extrapolated from the observed electric field values in the 512- to 1024-Hz band, can be  $\sim 10$  mV/m or higher. These strong electric fields generated in the ionosphere by lightning at local evening times may be important for the equatorial electrodynamic of the ionosphere.

### 1. Introduction

Unusual observations of an enhanced rate of impulsive signals observed during equatorial crossings of the Dynamics Explorer 2 (DE 2) satellite are interpreted as the result of equatorial focusing of lightning-generated whistler waves in the upper ionosphere at low altitudes during local evening hours.

Although whistlers have been extensively observed at low-latitude ground stations (see *Hayakawa and Ohta* [1992] for a review), relatively few cases have been reported of satellite observations of whistlers at both low latitudes and low altitudes [*Scarabucci*, 1970; *Dantas*, 1972; *Bullough et al.*, 1975; *Hayakawa*, 1992]. One of the principal conclusions of ground-based whistler studies at low-latitude stations is that while some of the whistlers observed on the ground propagated in ducts, a nonducted propagation path is needed to explain the properties of a large number of low-latitude whistlers. This is primarily due to (1) the relatively high curvature of the low-latitude field lines, which requires unreasonably large enhancements ( $\sim 100\%$ ) in density to effectively guide the waves along the field lines, and (2) the requirement of a favorable ionospheric tilt at the duct entrance and exit (see the introduction of *Tanaka and Cairo* [1980] for a detailed discussion). Nonducted mode of propagation at low latitudes is supported by the observations of NPM transmitter signals at Hawaii (21.5°N, 158°W) and at Dunedin, New Zealand (46°S, 170°W) [*Thompson*, 1987]. In this

study, *Thompson* [1987] demonstrated that three different ray paths were possible given an electromagnetic pulse (spheric) in the conjugate hemisphere. The signal was found to arrive quickly (i.e., 15 ms) through the Earth/ionospheric waveguide, and much later (i.e., 550 ms), via ducted whistler mode emission through space. However, the signal was also observed to arrive at intermediate times (i.e., 70 ms), via a nonducted ray path that extended to altitudes of 700 km.

The polar orbiting OGO 4 satellite measurements at  $\sim 600$ - to 900-km altitudes near the geomagnetic equator exhibited erosion or defocusing of waves injected from the ground [*Scarabucci*, 1970; *Dantas*, 1972]. These observations were interpreted in terms of increased transmission loss of waves entering the ionosphere at low latitudes and the inability of rays injected at midlatitudes to bend sufficiently to reach the equator at low altitudes. Using data from the Ariel 4 satellite (apogee 599 km, perigee 485 km, inclination 83°), *Bullough et al.* [1975] and *Hayakawa and Ohta* [1992] have reported spectral characteristics and spatial distribution of whistlers as a function of local time. In general, these authors have also reported low occurrence of whistlers at low latitudes ( $<10^\circ$ ) at all local times (see Figure 6 of *Hayakawa and Ohta*, 1992)]. Another related study is observations of ground transmitter signals on the FR 1 satellite (750 km, polar circular orbit) [*Cerisier*, 1973]. The main conclusion of this study was that below  $L = 1.7$  only nonducted propagation of signals injected from the ground takes place. Also using data from the FR 1 satellite, *Tanaka and Cairo* [1980] found large latitudinal variations of the wave normal direction of ground transmitter signals (NBA, 24 kHz) at low latitudes ( $<15^\circ$ ) in the evening sector and explained them by means of ray tracing simulations in the presence of an equatorial density anomaly.

Copyright 1995 by the American Geophysical Union.

Paper number 94JA02756.  
0148-0227/95/94JA-02756\$05.00

In a study of INJUN 3 satellite (apogee 2785 km, perigee 237 km) data, Gurnett [1968] reported wideband ELF/VLF observations in the altitude and latitude ranges of interest here, but the focus of his work was VLF hiss. However, as can be seen in Figure 3 of Gurnett [1968], whistlers observed in the 0- to 6-kHz band at  $<10^\circ$  latitude,  $<300$  km altitude and 1924 LT are consistent with the observations reported in the present paper.

In this paper, we provide an interpretation for a new set of observations involving an enhanced rate of impulsive electric field bursts observed at low altitudes (300-500 km) near the geomagnetic equator in the early evening sector around 1800-2000 MLT, first reported by Aggson *et al.* [1992]. Our interpretation is based on the focusing of nonducted whistler wave energy by the equatorial anomaly and is supported by results (reported here) of analysis of up to 61 passes of the DE 2 satellite during which these events were observed. The phenomenon is global in the sense that it is observed at all longitudes. Though the observation of an enhanced rate of spherics at low altitudes near the geomagnetic equator is in apparent contradiction with whistler-mode ELF/VLF wave propagation through a horizontally stratified ionosphere, we show that the presence of the equatorial anomaly with density peaks near  $\pm 20^\circ$  latitude in the evening sector provides the necessary focusing of waves to produce the observed effects.

The equatorial anomaly is a tropical ionospheric effect arising from equatorial electrodynamic [Kelley, 1989]. The zonal electric field at the magnetic equator is eastward during the day, which creates a steady upward  $\mathbf{E} \times \mathbf{B}/B^2$  plasma drift. Just after sunset this eastward field is enhanced, and the *F* region plasma can drift to very high altitudes, where recombination is slow, while the lower altitude plasma decays quickly once the sun sets. The result is something of a fountain effect, since the dense equatorial plasma rises until the pressure forces are high enough that the plasma starts to slide down the magnetic field lines, assisted by gravity, toward the tropical ionosphere. The net effect is essentially the formation of a ductlike structure with enhanced density along a field line near  $\pm 20^\circ$  geomagnetic latitude [Lockwood and Nelms, 1964; Tanaka and Cairo 1980].

The plan of the paper is as follows. In section 2 we describe the vector electric field instrument (VEFI), followed by the data set in section 3, with a summary of the initial observations reported by Aggson *et al.* [1992] and the results of our analysis of data from 61 different DE 2 passes. The interpretation of the observations is presented in section 4, and in section 5 we summarize our results and discuss the geophysical significance of this new phenomenon.

## 2. Experimental Method

### The Dynamics Explorer 2 Satellite

The Dynamics Explorer Program was designed to investigate coupling and interaction between the hot plasmas of the magnetosphere and the cooler plasmas of the plasmasphere, ionosphere, and upper atmosphere [Hoffman and Schmerling, 1981]. Both the high-altitude DE 1 and the low-altitude polar DE 2 satellites were launched and began measurements in 1981, with DE 2 reentering in 1983 and DE 1 discontinuing operations in 1991. The DE 2 satellite was in a polar orbit with an initial apogee and perigee of 1300 km and 305 km, respectively, and with a period of 101 min [Hoffman and Schmerling, 1981]. The DE 2 *Z* axis was usually along the orbit normal, the spacecraft *Y* axis was always held parallel or antiparallel to nadir, and the spacecraft *X* axis was determined by the right-hand rule and in the approximate direction of the velocity vector. During November 1981, DE 2 perigee was located near the

geomagnetic equator, which allowed measurements at both the low altitudes and low latitudes discussed in this paper.

### Vector Electric Field Instrument

The VEFI was designed to provide large dynamic range, high temporal/spatial resolution, and triaxial electric field measurements. Six 11-m-long cylindrical antennas were planned to be deployed along three axes to form an array, with the *Z* antenna along the spacecraft *Z* axis and the *X* and *Y* antennas at  $45^\circ$  to the spacecraft's *X* and *Y* axes, respectively. In orbit, however, one *Z* axis antenna failed to deploy, and measurements were limited to the *X* and *Y* electric field axes. The ac electric field measurements were performed in a  $1 \mu\text{V/m}$  to 10 mV/m range. The ac portion of the VEFI was composed of a filter bank of 20 channels, separated into two groups of eight channels covering the frequency range from 4 Hz to 1 kHz and one group of four channels covering from 1 kHz to 512 kHz. Quantitative spectral plots for all of the channels on a given orbit were obtained using three comb filter spectrometers. For the 16 channels between 4 Hz and 1 kHz (spectrometers A and B), both peak and rms values were recorded either once or twice per second, while for the four VLF channels from 1 kHz to 512 kHz (spectrometer C), only rms values were recorded either once or twice per second. In the spectrometer's high gain setting, sensitivity was approximately  $1 \mu\text{V/m}$  (independent of filter bandwidth), while in the low gain setting, sensitivity was approximately  $10 \mu\text{V/m}$  (See Table 1 of Maynard *et al.* [1981]). The general mode of operation of the VEFI was to assign spectrometers A and C to the axis nearest to perpendicular to the magnetic field. Spectrometer B was generally assigned to the axis nearest to parallel to the magnetic field. The detailed electric field observations presented here are from spectrometer B, channel 8 (512-1024 Hz) of the VEFI instrument.

The plasma density data presented here were obtained from the Langmuir probe on the DE 2 satellite [Krehbiel *et al.*, 1981].

## 3. Observations

The polar orbiting DE 2 spacecraft passes through the nightside equatorial region every 98 min at an altitude between 309 and 1012 km. We present here results of our analysis of data from 61 orbits during November 1981, when DE 2 passed over the geomagnetic equator between 300- and 500-km altitude around 1830-2000 LT. The first observations of the phenomenon discussed here were reported by Aggson *et al.* [1992]. On nearly every passage through the geomagnetic equator, impulsive signals are observed between few tens of Hz and a few kHz. An example is shown in Figure 1, which displays the peak electric field intensity as a function of the geomagnetic latitude for three typical orbital passes in the 512- to 1024-Hz band channel. In each case, as the spacecraft passed within  $\pm 15^\circ$  of the magnetic equator, peak emission levels are enhanced by nearly 40 dB. Based upon comparison with averaged electric field values obtained in the same interval, the signals are believed to be burstlike with a temporal duration of about 50 ms.

Figure 2 shows the observations of burst emissions in eight frequency channels (covering a frequency range of 4 Hz to 1024 Hz) of spectrometer B. We note that the rate of occurrence and strength of the signals are largest in the 512- to 1024-Hz channel, and very few or no signals are detected in the four lower channels (covering a frequency range of 4 Hz to 128 Hz).

Figures 3a, 3b, and 3c show the electric field intensity in 512-1024 Hz channel, plasma density values, and the *z* component of the dc electric field, respectively, during the DE 2 dip equator crossing occurring on November 15, 1981. The decrease in electron density

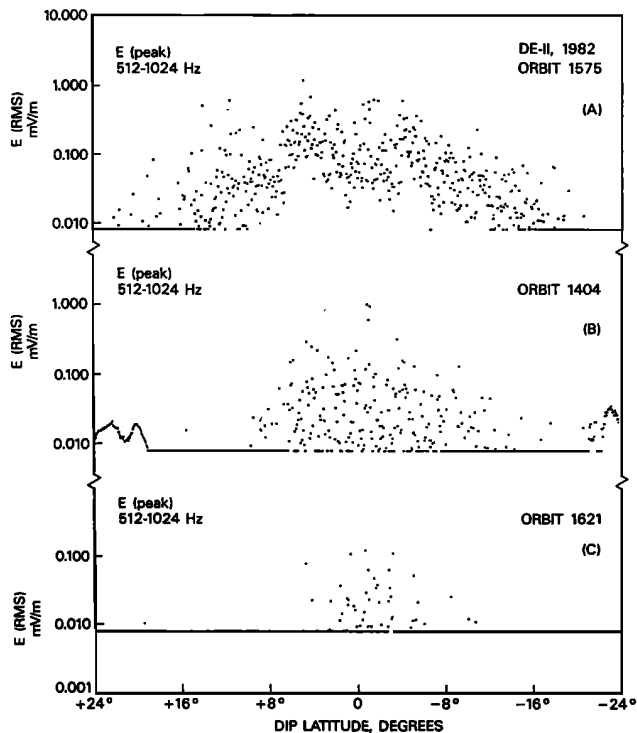


**Figure 1.** Three examples of DE 2 observations of impulsive signals near the geomagnetic equator in the 512- to 1024-Hz channel of the VEFI instrument.

and the dc electric field are indicative of the equatorial anomaly [Aggson *et al.*, 1987]. Note that the spheric bursts are centered about the dip equator and they occur while the spacecraft is near the central region of the equatorial anomaly.

The salient features of our observations based on the analysis of wave (1 s sampling period) and plasma data from 61 DE 2 orbits are as follows.

1. The 512- to 1024-Hz channel showed impulsive signals peaking near the geomagnetic equator in 57 out of 61 nightside equator crossings. The latitude range around the geomagnetic equator over which these impulsive signals were observed varied between 5 and 20°. Though the peak of the activity was found to be close to the equator, the signal activity was often distributed asymmetrically in latitude around the geomagnetic equator. In general, impulsive signals were observed more frequently over a larger latitude range in the southern hemisphere.

2. Burstlike signals peaking near the geomagnetic equator were also observed in 181-256, 256-361, and 361-512 Hz channels of spectrometer B and in channels of spectrometer A covering a similar frequency range. Very few or no signals were detected in lower frequency channels (covering 4-128 Hz). Burst signals were also detected in the 4- to 16-kHz channel of spectrometer C. However, the strongest and most frequent occurrences of signals were always detected in the 512- to 1024-Hz channel.

3. The peak intensity in the 512- to 1024-Hz band was generally  $\leq 1$  mV/m, the median value being a few hundred mV/m.

4. Impulsive signals were observed on equatorial passes at all longitudes.

5. The altitude of DE 2 during its geomagnetic equatorial crossings in the 61 cases was in the range of 300-500 km.

6. The impulsive emissions were detected between 1830 and 2000 MLT.

7. In all cases when impulsive events were detected by the VEFI instrument, the electron density data from the Langmuir probe showed a reduction in density near the geomagnetic equator and broad peaks near  $\pm 20^\circ$  invariant geomagnetic latitudes. The strongest impulsive electric field signals were always observed at a latitude close to the geomagnetic equator corresponding to the valley region in the electron density data.

#### 4. Interpretation

The signals in the 512- to 1024-Hz channel were interpreted to be impulsive (lasting tens of milliseconds) because of the observed high ratios between peak and rms values of the electric field data sampled once per second. Evidence of the wideband nature of the signals was the fact that they were simultaneously observed in 8-16 Hz, 512-1024 Hz, and 4-16 kHz channels. Based on the wideband and impulsive nature and frequency of occurrence of the signals, we interpret them as having originated in lightning discharges occurring at longitudes close to (within  $\pm 10 - 20^\circ$ ) those of the DE 2 satellite during the observation period.

Recent rocket measurements indicate the presence of nonducted ray paths at low altitudes near the geomagnetic equator. An example is shown in the frequency-versus-time radio spectrogram, Figure 4, obtained from the electric field experiment onboard the Kwajalein rocket (29.028) flying at 400-km altitude and near 8° magnetic latitude, i.e., within the same altitude and latitude discussed in this paper. Clearly evident in the figure are two closely spaced, highly dispersed whistlers extending from about 100 to 2400 Hz. Also present are their parent spheric signals observed between 25 and 1600 Hz. The parent spherics have only slight dispersion and last about  $\sim 50$  ms. The spherics have probably propagated by a nonducted path, and the dispersed whistlers either by a ducted path or by a magnetospherically reflected nonducted path. Both the spherics and whistlers, if observed by a receiver with narrowband frequency ( $\sim 500$  Hz) channels, would appear similar to the impulsive signals observed on DE 2 satellites described in this paper.

Our interpretation is in sharp contrast to previous OGO 4 (apogee 900 km, perigee 400 km) daytime observations of whistlers near the geomagnetic equator reported by Scarabucci [1970]. He found (1) a decrease in the upper cutoff of whistlers as the satellite approached the geomagnetic equator, and (2) a decrease in signal intensity as the satellite approached the geomagnetic equator, and sometimes complete loss of signal as its intensity dropped below the instrument threshold. Those observations were explained satisfactorily in terms of ionospheric transmission loss as a function of latitude and frequency and the accessibility to the satellite location of rays entering the horizontally stratified ionosphere from a subionospheric region.

To put our interpretation in the proper context, we review briefly the reasons for low occurrence rates and low intensities at low altitudes near the geomagnetic equator, as observed by Scarabucci [1970], Dantas [1972], and Hayakawa and Ohta [1992]. Figure 5 shows ionospheric transmission loss as a function of latitude and frequency under daytime conditions [Scarabucci, 1970]. The higher frequencies suffer relatively greater losses, and both the amount of loss and its frequency dependence increase rapidly toward lower latitudes. During evening and nighttime, losses are reduced because of lower *D* region absorption, but the dependence of losses on frequency and latitude remains generally the same [Hayakawa, 1992]. Note that at all frequencies, transmission loss increases monotonically with decreasing latitude.

With this background, we now simulate the propagation through the ionosphere using ray tracing. A diffusive equilibrium model is

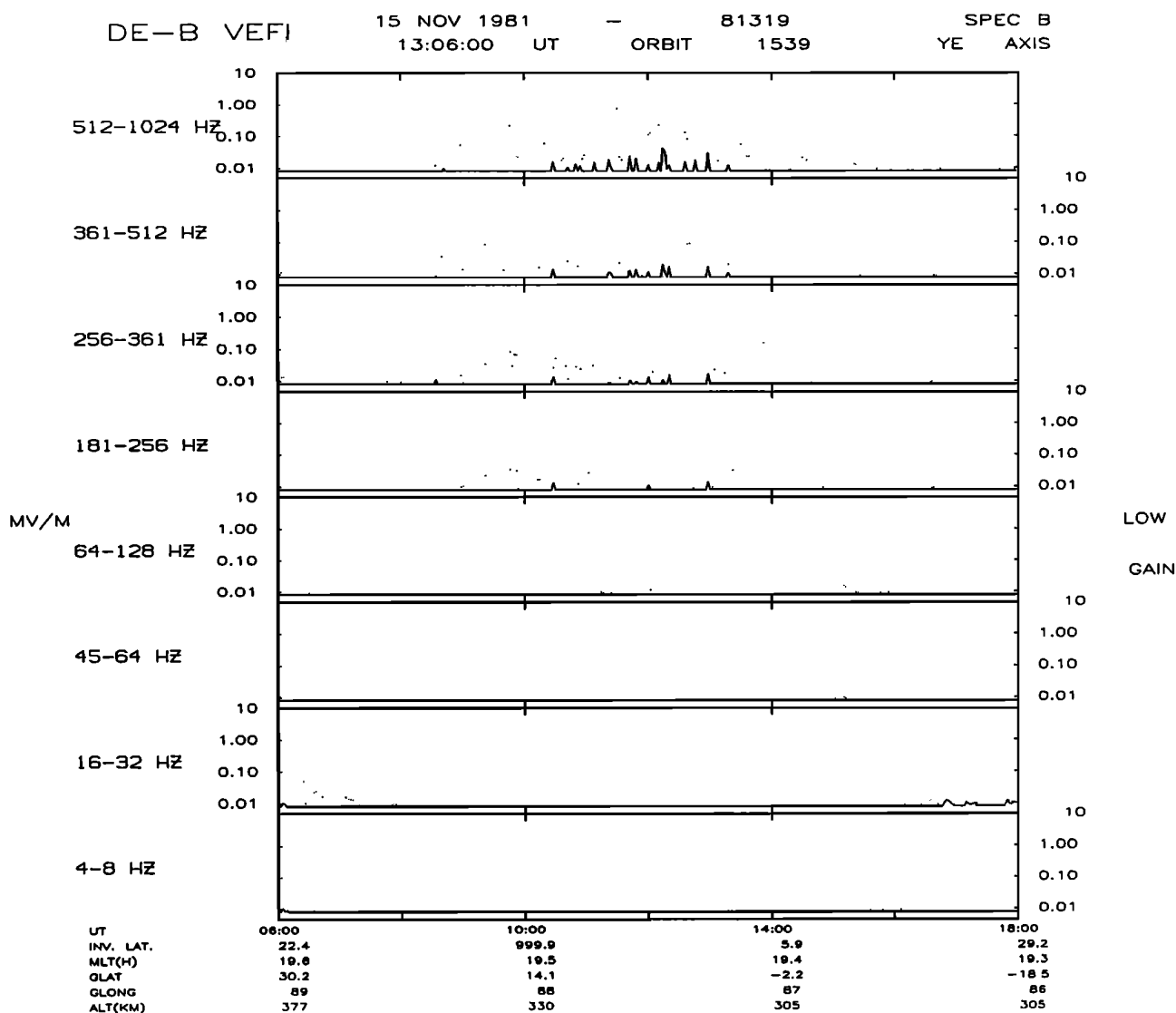
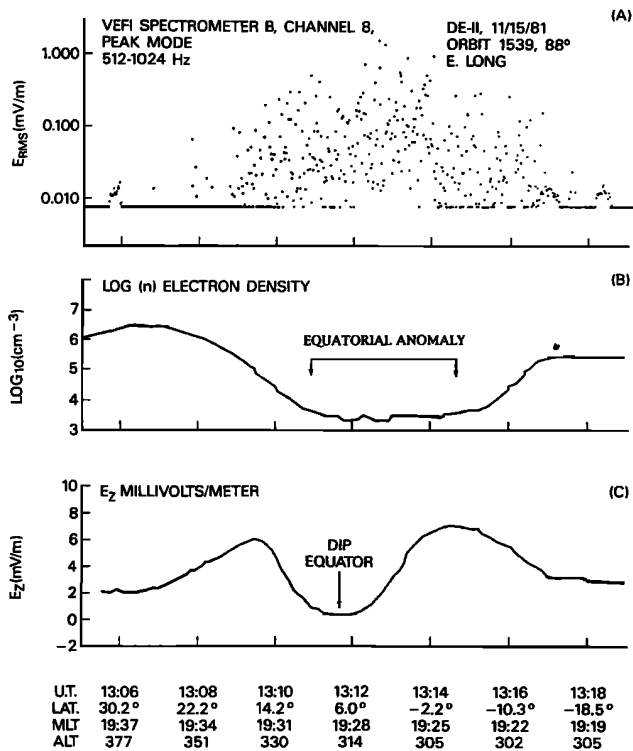


Figure 2. An example of data from eight channels (covering 4-1024 Hz) of spectrometer B. The impulsive emissions are detected primarily in the four higher-frequency (181-1024 Hz) channels.

used, characterized at 500 km by the following parameter values: ionic composition 89.8%  $O^+$ , 9.8%  $He^+$ , 0.4%  $H^+$ , isothermal electron and ion temperature 1000°, and electron density  $1.5 \times 10^5/cm^3$  [Prasad, 1968]. Figure 6a shows the equatorial electron density as a function of radial distance for this model. Figure 6b shows rays (750-Hz frequency) injected at 200 km at various starting latitudes in a horizontally stratified ionosphere, and with vertical initial wave normals. Also shown is a typical DE 2 trajectory in November 1981 as it crossed the geomagnetic equator. Taking the results from Figures 5 and 6b together, we expect the signal intensity observed on DE 2 to decrease as the satellite approaches the geomagnetic equator. Near the equator, only rays entering the ionosphere in the 5-10° latitude range would reach the satellite altitude, and as shown in Figure 5, waves entering at these low latitudes would suffer large transmission loss. The lack of impulsive signals in this case is consistent with the report by OGO 4 investigators, and is the situation expected on the dayside. A further reduction in the intensity of signals entering at low latitudes comes from the loss incurred in Earth-ionosphere waveguide propagation. This loss at

1 kHz is about 20 dB over 500-km distance and 40 dB over 2000 km [Crary, 1961]. Thus for lightning discharges taking place at 15-20° geomagnetic latitude, waves entering the ionosphere at low latitudes would suffer this additional loss. Thus, based on the assumption of horizontal ionospheric stratification, we expect to see a minimum in the whistler activity observed on the DE 2 satellite near the geomagnetic equator, in contradiction of the observations of enhanced impulsive signal rate and intensity discussed above.

The disagreement between ray tracing modeling and observations is resolved when we consider the presence of the equatorial density anomaly. To include the anomaly in our raytracing analysis, we interpret the observed double-peaked electron density distribution (Figure 3b) to represent a sample of the equatorial anomaly along the DE 2 orbit. This interpretation is consistent with past topside sounding observations of a double-peaked equatorial anomaly observed in the local evening sector [Lockwood and Nelms, 1964; Goodall et al., 1975]. We now present ray tracing simulations of waves injected from subionospheric sources through the evening ionosphere that includes the equatorial density anomaly. The back-



**Figure 3.** (a) DE 2 observations of impulsive signals near the geomagnetic equator in the 512- to 1024-Hz channel of the VEFI instrument. (b) Langmuir probe observations of electron density illustrating equatorial (Appleton) anomaly. (c) The  $z$  component of dc electric field associated with the anomaly.

ground ionospheric density profile used is the same as noted above. The anomaly is modeled as a whistler duct with 500% enhancement and a half width of  $\Delta L \cong 0.08$  along the geomagnetic field at  $18.5^\circ$  invariant latitude. The duct factors are chosen so as to correspond to the anomaly model LG-18.34 of *Tanaka and Cairo* [1980]. Those authors have shown that this model is in good agreement with the experimental results obtained during the most strongly developed phase of the anomaly in the evening time [Lockwood and Nelms, 1964; Goodall et al., 1975]. DE 2 ion density data show that equatorial anomalies observed during the evening times in November 1981 have characteristics similar to that observed by these authors. Figure 7a shows the assumed variation of electron density profile at 400 km altitude as a function of latitude. The equatorial anomaly manifests itself as increased electron density near  $20^\circ$  latitude. The net effect of the anomaly is to introduce horizontal density gradients in the ionosphere, which bend the rays equatorward much more rapidly with distance along the ray path than would be the case in the absence of the anomaly. Rays injected at latitudes  $< 30^\circ$  thus reach the equator at relatively low altitudes after one or more reflections from the lower ionosphere. Figure 7b shows the results of ray tracing analysis and the DE 2 satellite trajectory. Rays at 750 Hz were injected at  $5^\circ, 10^\circ, 15^\circ, 20^\circ, 25^\circ, 30^\circ,$  and  $35^\circ$  latitude and at 200-km altitude with vertical wave normal directions. We observed four general features of the ray paths shown.

1. Unlike the typical dayside profile, the equatorial anomaly allows rays injected from as far as  $\sim 30^\circ$  latitude to be focused and observed at the equator at low altitudes. As described in Figure 5, rays launched from below  $\sim 10^\circ$  latitude suffer severe transmission loss. However, those launched from higher latitudes should pass with minimal losses.

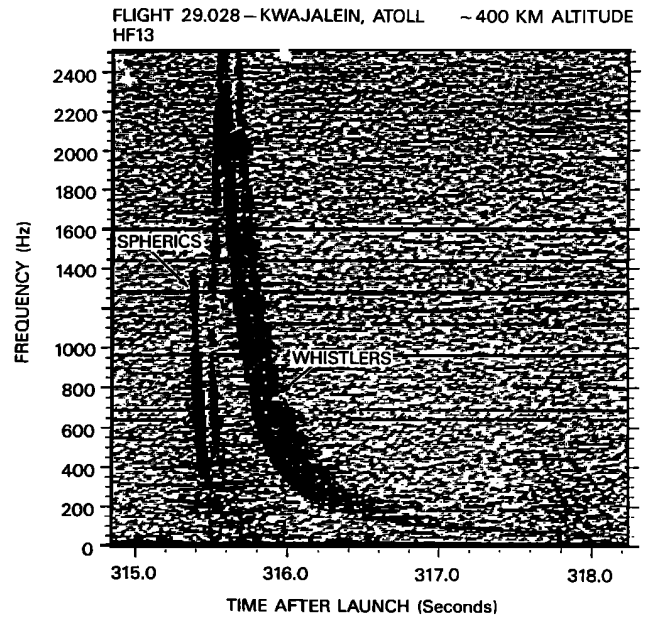


**Figure 4.** Rocket observations of ducted and nonducted propagation of whistlers.

2. There is a concentration of ray paths near the equator.
3. Rays remain confined to relatively low altitudes of  $< 800$  km.
4. The region populated by the rays is asymmetrically positioned with respect to the geomagnetic equator with the rays covering a wider latitude range in the hemisphere of the source.

We note here that the above-noted qualitative features of our results are not strongly dependent on the parameters of the equatorial anomaly, for example, the invariant latitude of the field line of the anomaly and the enhancement factor. Features 1, 2, and 3 of ray

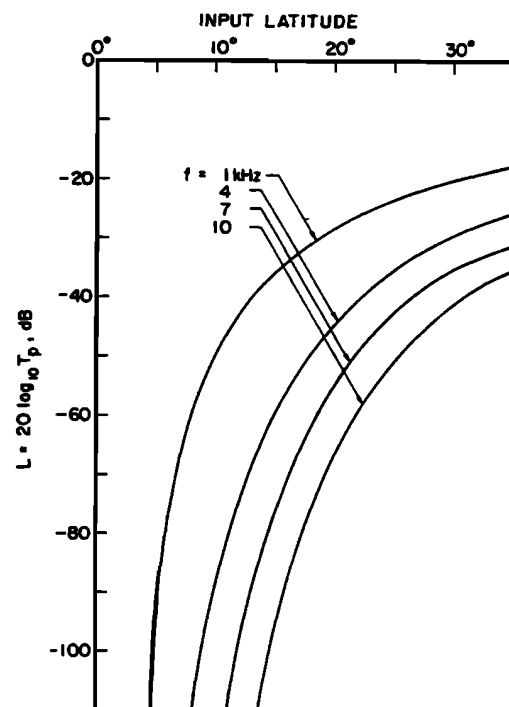


**Figure 5.** Total ionospheric loss (reflection plus absorption) as a function of magnetic latitude for several frequencies [Scarabucci, 1970].

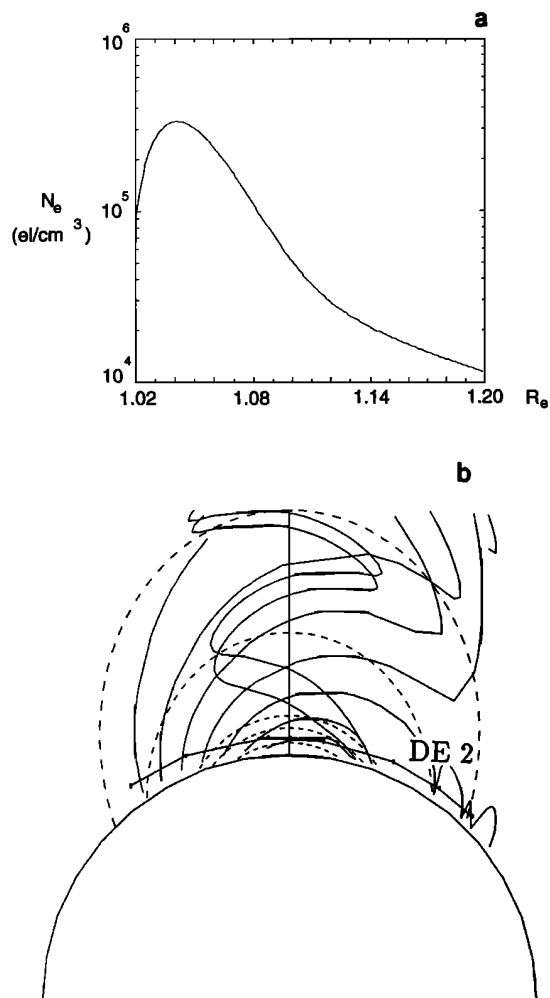


**Figure 6.** Ray tracings through a horizontally stratified ionosphere. (a) Equatorial electron density as a function of radial distance. (b) Trajectories of rays (750 Hz frequency) injected at 200-km altitudes with vertical wave normal angles.

tracing simulations are consistent with the main features of the data, that strong whistler activity is observed at low geomagnetic latitudes with a peak near the geomagnetic equator. Feature 4 is consistent with the asymmetry observed in the data with respect to latitudinal distribution around the equator if we assume lightning to occur more often in the southern hemisphere. As shown in Figure 8, this latter assumption is consistent with optical observations of lightning in November at dusk from the DMSP satellite, which shows that most of the lightning at this local time takes place in the southern hemisphere [Turman and Edgar, 1982]. Furthermore, it is found that the longitudinal distribution of the satellite trajectories for which the impulsive signals were observed tended to concentrate over regions where lightning activity peaks in November at dusk time (Figure 8). That the observations were during dusk (1800 to 2000 MLT) is also consistent with previous data on the strong equatorial anomaly with double peaks developing soon after sunset [Lockwood and Nelms, 1964; Goodall et al., 1975].

To estimate dispersion in the 512- to 1024-Hz channel (and thus the duration of the bursts), ray tracing simulations were carried out for waves at different frequencies in the 500- to 1000-Hz range, with rays injected vertically at 200 km at various latitudes. Since data were collected once every second, group delays of various rays

reaching the same satellite location within  $\sim 10$  km (distance covered by the satellite in 1 s) were compared to estimate the dispersion. We found that typically, rays with a wave frequency between 700 and 900 Hz (injected at approximately the same latitude) reached the satellite location within 10 km. The dispersion determined from ray tracing simulation was found to be of the order of 50-100 ms, consistent with the burst duration of 50 ms estimated by comparing peak and average electric fields. For example, the dispersion for rays injected near  $20^\circ\text{N}$  geomagnetic latitude, and reaching the satellite altitude (400 km) near the geomagnetic equator ( $-7.3^\circ\text{S}$ ) after  $\sim 2$  s of average group delay, was  $< 50$  ms.

Ray tracing simulations permit estimation of the burst magnetic field value. At 800 Hz, rays injected near  $20^\circ$  geomagnetic latitude reach the equator with a wave refractive index of  $\sim 1000$  and a wave normal angle of  $\sim 88^\circ$ . Using the whistler-mode polarization relations, we estimate the wave magnetic field of the order of a few hundred pT, corresponding to a burst electric field of 1 mV/m in the 512- to 1024-Hz channel. Thus a low altitude satellite equipped with a magnetic sensor (typically used for plasma wave measurements) can easily detect these bursts.

The lack of burst signals below  $\sim 100$  Hz can be due to low frequency cutoff that exists for whistler mode signals when more than one dominant ion species are present [Smith and Brice, 1964].

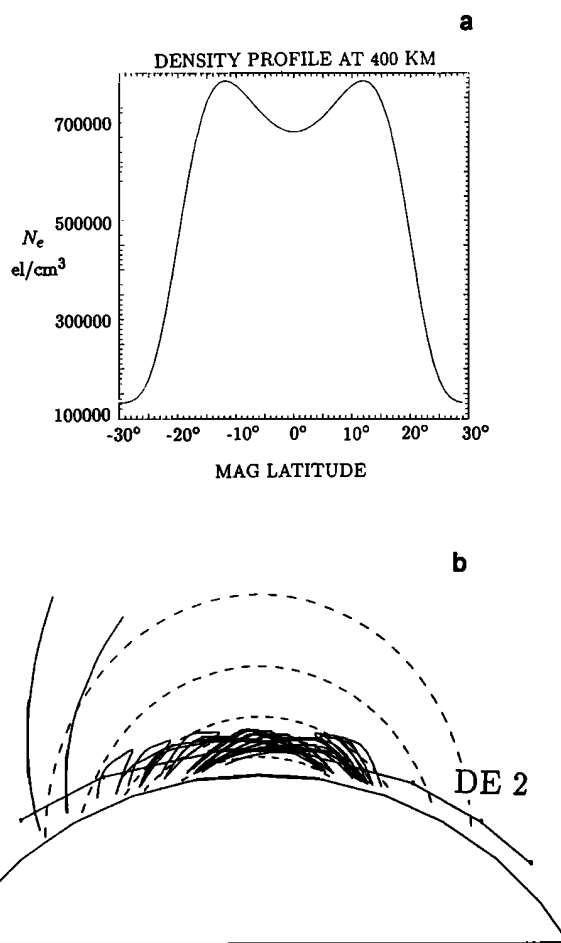


**Figure 7.** Ray tracings in the presence of an equatorial anomaly. (a) Electron density at 400-km altitude as a function of latitude. (b) Trajectories of rays (750 Hz frequency) injected at 200-km altitudes with vertical wave normal angles.

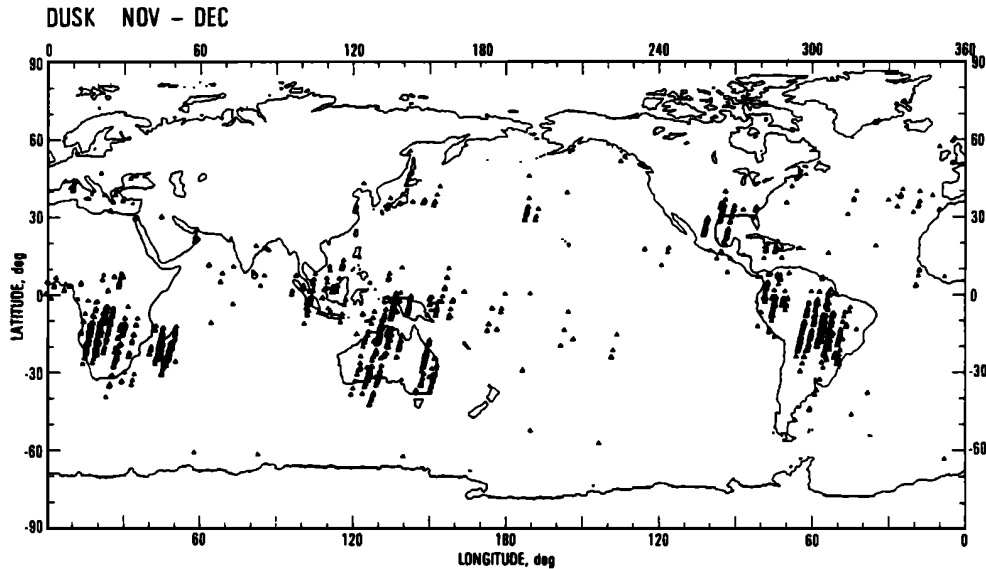


**Figure 8.** Lightning activity observed by Defense Meteorological Satellite Program (DMSP) satellite at dusk during November and December 1977 [Turman and Edgar, 1982].

The two-ion whistler mode cutoff frequency  $f_{2Ic}$  for an ionospheric plasma with  $O^+$  and  $He^+$  dominant ions is given by

$$f_{2Ic} = f_H \left( \frac{A_{He^+}}{M_{O^+}} + \frac{A_{O^+}}{M_{He^+}} \right), \quad (1)$$

where  $f_H$  is the electron gyrofrequency,  $A_{He^+}$  and  $A_{O^+}$  are the fractions of charge density occupied by  $He^+$  and  $O^+$  respectively, and  $M_{He^+}$  and  $M_{O^+}$  are the mass to charge ratio of  $He^+$  and  $O^+$  respectively relative to that of the electron. For ionospheric plasma at 200 km composed primarily of 90%  $O^+$  and 10%  $He^+$ , we obtain  $f_{2Ic} = 185$  and 215 Hz at  $0^\circ$  and  $20^\circ$  latitude, respectively. We note here, however, that some of the wave energy below  $f_c$  can couple into whistler mode via a mode coupling process [Wang, 1971; Rodriguez and Gurnett, 1971].

The observation of the strongest and most frequent signals in the 512- to 1024-Hz band is likely to be a manifestation of the combined effects of the shape of lightning radiation spectra and ionospheric transmission loss as a function of frequency. Lightning spectra in the ELF/VLF range generally peak in the few-kHz range and are relatively flat down to  $\sim 1$  kHz, after which they drop sharply [Bliokh et al., 1980]. Thus higher ionospheric transmission loss at higher frequencies would tend to reduce the intensity of signals above the 512- to 1024-Hz range. At lower frequencies ( $< 500$  Hz), lightning energy is down by about  $\sim 20$  dB compared to the level at 1 kHz; thus the reduced intensity of impulsive signals at lower frequencies.

## 5. Summary and Discussion

DE 2 observations near the geomagnetic equator in evening hours appear to be interpretable as enhanced nonducted whistler activity resulting from increased access for VLF ray paths to satellite altitudes due to the presence of the equatorial anomaly. This phenomenon is observed at all longitudes and, in that sense, is global. All observed characteristics can be explained in terms of propagation of ELF/VLF wave energy from lightning discharges in the presence of the double-peaked equatorial anomaly that develops during the early evening hours, soon after sunset. In essence, waves injected at latitudes  $< 30^\circ$  are trapped in that part of the equatorial ionosphere

bounded by the field lines along which enhanced plasma density is observed. The variability observed in the phenomenon from case to case can be understood in terms of the variability in the lightning activity and in the characteristics of the equatorial anomaly. The four cases when whistlers were not detected can probably be explained in terms of the absence of thunderstorm activity near the satellite longitudes at the time of the observations. We suggest that with a more detailed quantitative analysis of the phenomenon, it may be possible to use data from low-altitude satellites to monitor thunderstorm activity as well as the equatorial anomaly.

The realization of this new means by which radio energy from lightning populates the magnetosphere may have potential geophysical significance, especially in the context of other results. Several recent studies indicate that electromagnetic energy released in worldwide lightning discharges may significantly influence the Earth's ionosphere and magnetosphere. It has been shown that lightning-generated whistlers can precipitate electrons from the radiation belts, and these electrons can enhance the plasma density in the lower ionosphere via secondary ionization [Voss et al., 1984; Inan et al., 1990]. Lightning can heat and ionize the lower ionosphere through direct electromagnetic coupling [Inan et al., 1991]. Whistlers generate lower hybrid waves that can accelerate thermal  $H^+$  ions to  $\sim 40$  eV [Bell et al., 1991, 1993] and hiss that is believed to be responsible for the slot region in the radiation belts [Sonwalkar and Inan, 1989; Draganov et al., 1992; Lyons et al., 1972]. The observations presented here indicate that during certain hours in the evening, almost all the energy input from lightning discharges entering the ionosphere at  $< 30^\circ$  latitude remains confined to a small region (in altitude and latitude) near the geomagnetic equator. The net wideband electric field, extrapolated from the observed electric field values in the 512- to 1024-Hz band, can be  $\sim 10$  mV/m or higher. These strong electric fields generated in the ionosphere by lightning at local evening times may be important for the equatorial electrodynamics of the ionosphere. For instance, these fields can possibly heat ions by the mechanisms recently suggested by Bell et al. [1991, 1993]. Furthermore, rather large values ( $\sim 10$  mV/m) of whistler electric fields in the equatorial region indicate that nonlinear effects will be important.

**Acknowledgments.** We gratefully acknowledge the helpful comments of D. L. Carpenter and R. A. Helliwell on the manuscript. This work was supported by NASA grant NAG5-1549.

The Editor thanks R. D. Hunsucker and another referee for their assistance in evaluating this paper.

## References

- Aggson, T. L., N. C. Maynard, F. A. Herrero, H. G. Mayr, L. H. Brace, and M. C. Liebrecht, Geomagnetic equatorial anomaly in zonal plasma flow, *J. Geophys. Res.*, **92**, 311, 1987.
- Aggson, T. L., J. DeConde, W. M. Farrell, M. D. Desch, R. Pfaff, U. S. Inan, and V. S. Sonwalkar, M. Liebrecht, Observation of spheric-like noise at satellite altitudes near the magnetic dip equator, (abstract) *Eos, Trans. AGU*, **73**(43), Fall Meeting suppl., 415, 1992.
- Bell, T. F., R. A. Helliwell, and M. K. Hudson, Lower hybrid waves excited through linear mode coupling and the heating of ions in the auroral and subauroral magnetosphere, *J. Geophys. Res.*, **96**, 11,379, 1991.
- Bell, T. F., R. A. Helliwell, U. S. Inan, and D. S. Lauben, The heating of suprathermal ions above thunderstorm cells, *Geophys. Res. Lett.*, **20**, 1991, 1993.
- Bliokh, P. V., A. P. Nicholaenko, and Yu. F. Fillippov, *Schumann Resonances in the Earth-Ionosphere Cavity*, Institute of Electrical Engineers, New York, 1980.
- Bullough, K., M. Denby, W. Gibbons, A. R. W. Hughes, T. R. Kaiser, and A. R. L. Tatnall, E.I.f./v.l.f. emissions observed on Ariel 4, *Proc. R. Soc. London, A*, **343**, 207, 1975.
- Cerisier, J. C., A theoretical and experimental study of non-ducted VLF waves after propagation through the magnetosphere, *J. Atmos. Terr. Phys.*, **35**, 77, 1973.
- Crary, J. H., The effect of the Earth-ionosphere waveguide on whistlers, *Tech. Rep. 9*, Stanford Electron. Lab., Stanford, Calif., 1961.
- Dantas, N. H., OGO 4 satellite observations of whistler-mode propagation effects associated with caustics in the magnetosphere, *Tech. Rep. 3469-1*, Stanford Electron. Lab., Stanford, Calif., 1972.
- Draganov, A. B., U. S. Inan, V. S. Sonwalkar, and T. F. Bell, Magnetospherically reflected whistlers as a source of plasmaspheric hiss, *Geophys. Res. Lett.*, **19**, 61, 1992.
- Goodall, C. V., H. D. Hopkins, Y. Kabasakal Tulunay, and R. J. D'Acry, Topside ionosphere electron density measurement on Ariel 4, *Proc. R. Soc. London, A*, **343**, 189, 1975.
- Gurnett, D. A. Observations of VLF hiss at very low  $L$  values, *J. Geophys. Res.*, **73**, 1096, 1968.
- Hayakawa, M., Satellite observation of low-latitude VLF radio noises and their association with thunderstorms, *J. Geomagn. Geoelectr.*, **41**, 573, 1989.
- Hayakawa, M., and K. Ohta, The propagation of low-latitude whistlers: a review, *Planet. Space Sci.*, **40**, 1339, 1992.
- Hoffman, R. A., and E. R. Schmerling, Dynamics Explorer Program: An overview, *Space Sci. Instrum.*, **5**, 345, 1981.
- Inan, U. S., F. A. Knifsend, and J. Oh, Subionospheric VLF imaging of lightning-induced electron precipitation from the magnetosphere, *J. Geophys. Res.*, **95**, 17217, 1990.
- Inan, U. S., T. F. Bell, and J. V. Rodriguez, Heating and ionization of the lower ionosphere by lightning, *Geophys. Res. Lett.*, **18**, 705, 1991.
- Kelley, M. C., *The Earth's Ionosphere*, Academic, San Diego, Calif., 1989.
- Krehbiel, J. P., L. H. Brace, R. F. Theis, W. H. Pinkus, and R. B. Kaplan, The Dynamics Explorer Langmuir probe instrument, *Space Sci. Instrum.*, **5**, 493, 1981.
- Lockwood, G. E. K., and G. L. Nelms, Topside sounder observations of the equatorial anomaly in the 75°W longitude zone, *J. Atmos. Terr. Phys.*, **26**, 569, 1964.
- Lyons, L. R., R. M. Thorne, and C. F. Kennel, Pitch angle diffusion of radiation belt electrons within the plasmasphere, *J. Geophys. Res.*, **77**, 3455, 1972.
- Maynard, N. C., E. A. Bielecki, and H. F. Burdick, Instrumentation for vector electric field measurements from DE-B, *Space Sci. Instrum.*, **5**, 523, 1981.
- Prasad, S. S., Nighttime ionic composition and temperature over Arecibo, *J. Geophys. Res.*, **73**, 6795, 1968.
- Rodriguez, J. V. P., and D. A. Gurnett, An experimental study of Very-Low-Frequency mode coupling and polarization reversal, *J. Geophys. Res.*, **76**, 960, 1971.
- Scarabucci, R. R., Satellite observations of equatorial phenomena and defocusing of VLF electromagnetic waves, *J. Geophys. Res.*, **75**, 69, 1970.
- Sonwalkar, V. S., and U. S. Inan, Lightning as an embryonic source of VLF hiss, *J. Geophys. Res.*, **94**, 6986, 1989.
- Tanaka, Y., and L. Cairo, Propagation of VLF waves through equatorial anomaly, *Ann. Geophys.*, **36**, 555, 1980.
- Thompson, N. R., Ray-tracing the paths of very low latitude whistler-mode signals, *J. Atmos. Terr. Phys.*, **49**, 321, 1987.
- Turman, B. N., and B. C. Edgar, Global lightning distributions at dawn and dusk, *J. Geophys. Res.*, **87**, 1191, 1982.
- Voss, H. D., W. L. Imhof, J. Mobilia, E. E. Gaines, M. Walt, U. S. Inan, R. A. Helliwell, D. L. Carpenter, J. P. Katsufakis, and H. C. Chang, Lightning induced electron precipitation, *Nature*, **312**, 740, 1984.
- Wang, Ting-i, Intermode coupling at ion whistler frequencies in a stratified collisionless ionosphere, *J. Geophys. Res.*, **76**, 947, 1971.

T. L. Aggson, W. M. Farrell, and R. Pfaff NASA Goddard Space Flight Center, Greenbelt, MD 20771.

U. S. Inan, and V. S. Sonwalkar, STAR Laboratory, Stanford University, Durand 319, Stanford, CA 94305-4055.

(Received August 30, 1994; revised October 17, 1994; accepted October 19, 1994.)